Title: Measurements of Fuel Adhesion on Cylinder Walls and Fuel Wall-flow Behavior with Post Diesel Fuel Injections

Author: Gen Shibata, Shogo Nishiuchi, Puqing Xie, Shuntaro Takai, Hideyuki Ogawa, and Yoshimitsu Kobashi

Abstract

Post fuel injection in the expansion stroke is used for diesel particulate filter (DPF) regeneration, however, fuel spray impinges on the cylinder liner due to the low temperature and pressure conditions. Fuel adhesion and fuel flowing down across the cylinder liner, the so-called “wall-flow”, was observed by high speed video images, and this adhesion is a cause of diesel engine lubricant oil dilution and the deterioration of fuel consumption in diesel engines. In this paper, the fuel adhesion and the wall-flow of post diesel fuel injections were investigated with a high pressure-temperature constant volume optical chamber. The in-cylinder temperatures and pressures at 30, 60, and 90 °CA ATDCs, conditions commonly employed in post fuel injection timings, were measured by an actual engine, and similar conditions were created in the constant volume chamber by the combustion of a pre-mixed gas of ethylene, oxygen, and nitrogen. Fuel masses of 0.6 mg, 1.1 mg, and 1.7 mg per hole were injected at each ATDC setting. The weight of the adhered fuel on the wall and the fuel in the piston-cylinder crevice were measured by precision balance, and the liquid-vapor phases in the spray were observed by Mie scattering and shadowgraph methods. To measure the thickness of the adhered fuel on the cylinder wall, the LIF method was employed. The results show that the fuel spray penetration and adhesion on the cylinder wall were different in the test conditions investigated here. With the early post injection, most of the injected fuel vaporizes without penetrating to the cylinder liner and gaseous diesel fuel is condensed on the cylinder wall. A thin and widely spread out fuel film is formed on the cylinder wall, however no wall-flow could be confirmed by the high speed video images. With late post fuel injections, the strong penetration of liquid fuel reaches the cylinder wall, and a thick and widely spread out fuel film was formed on the cylinder wall and the wall-flow phenomenon was observed here, however the quantity of fuel involved in the wall-flow was smaller than that of the fuel adhering to the cylinder wall.

The effects of in-cylinder pressure and temperature on the fuel adhesion on the cylinder wall were investigated. With the increase of pressure and temperature, the quantity of adhering

fuel was reduced, suggesting that the boost pressure increase by turbo charging and a higher engine load is effective to reduce fuel adhesion.

Further, the effects of multiple post fuel injections on fuel adhesion to the cylinder wall were investigated, maintaining the total fuel injection amounts. With increases in the number of fuel injections, the total percentage of adhering post fuel on the cylinder wall was reduced. In the multiple fuel injections, it was observed that fuel motion takes place during the spray pass after the first and second fuel injections, and that the penetration length of the second and third fuel sprays increases.

Introduction

To capture the particulate matter (PM) in the diesel engine exhaust gas, a diesel particulate filter (DPF) is attached to recent diesel vehicles. As the PM on the DPF surface accumulates beyond some amount, the pressure rise between the inlet and outlet of the DPF increases, and this finally leads to a rise in the backpressure of the engine exhaust. To remove the PM and regenerate the DPF, post fuel is injected and oxidized by a DOC (Diesel oxidation catalyst) located upstream of the DPF, and the high temperature exhaust gas burns the PM [1], [2], as shown in Figure 1. However, due to the relatively low temperature and pressure in the cylinder after the main combustion, fuel spray with strong penetration impinges on the cylinder wall and some of the fuel adheres to the cylinder wall eventually to be scraped down by the piston rings into the crankcase [3].

Much research has been conducted into engine oil dilution by post fuel injection, and it can be classified into three types. First, engine oil sampling tests during the operation where the oil dilution rate is measured with or without post fuel injection. Here, Deconnicnck and Delvigne used radiotracer labeling to measure oil dilution rates [4]. Different from other research, the oil sampling is not directly from the engine but from a monitor chamber where the engine oil is circulated. The effect of oil and fuel properties on the oil dilution has been investigated by Oinuma and Takuma [5]. The oil dilution was detected immediately after the fuel injection by measuring the friction between piston ring and cylinder wall. It showed that high viscosity oil has poorer dilution characteristics, and that increasing injection pressure as well as advanced post injection timings suppress oil dilution. The research conducted by Wattrus reported that the viscosity, density, and tension affect the oil dilution more than the final boiling point [6]. Parks and Partridge used a LIF (Laser-Induced Fluorescence) method to measure the oil dilution [7]. These experiments were conducted with various injection

strategies. The results showed that late fuel injection is a cause of higher oil dilution rates.

A second type of investigation is of the post fuel injection spray and wall impingement behavior, conducted with an optical constant volume chamber. In the research conducted by Katsura [8], diesel fuel was injected into a high temperature chamber, and high speed video images were recorded with transmitted and scattered light. Zhao [9] investigated diesel fuel spray impingement experimentally and numerically. A spray impingement model was developed and validated by Mie-scattering and schlieren observations. The effects of surface properties on the spray wall impingement behavior and fuel adhesion were reported by Ko Kyungnam [10]. The results show that the adhering quantity changes depending on the wall surface situations. The spray impingement on recessed walls occurred with a rolling up motion while the impingement on flat walls expanded along the wall surface in the radial direction. A rugged wall results in the most adhesion followed by that on recessed walls, and flat walls show the least adhesion. The effects of injection pressure on the liquid fuel film adhering on the walls were investigated by Maramutsu [11] by a LIF method. The results show that increases in the injection pressure reduce the quantity of liquid film adhesion, and the effects of ambient density, distance from nozzle to wall and injection pressure on the impinging spray.

A fuel film experiment was conducted by Yang to investigate the effect of ambient temperature, density, and nozzle diameter on the fuel film characteristics [12]. In the research conducted by Moller [13], the deposition of an impinging diesel spray was studied optically with a constant volume chamber under different ambient pressures. The effect of the impingement angle on the spray impingement behavior was investigated by Ebara and Amagai [14]. Here, a high-density zone was observed when the fuel spray impinged on the wall, and the location of the high-density zone varies with impingement angle changes. Spray to spray interactions were investigated by Amagai and Maruyama [15]. Different from a real engine, the sprays here were arranged in parallel and impingement was on a vertical wall. It was found that when two sprays interact the result is a swollen spray and this was observed to be caused by the interaction of the sprays. Further, the droplet behavior has also been investigated. In the research by Al-Roub [16], the droplet to droplet and droplet to liquid film interactions have been investigated. With liquid films formed in the saturation regime, liquid film breakup depends on the energy content of the impinging droplets, the level of the liquid film surface disturbance, and the liquid film thickness. In the transition and film boiling regimes, droplet numbers, the Weber number, and surface superheat affect the interaction

process.

The third group of reports investigates the spray wall impingement by simulation and estimates of engine oil dilution models based on the test data of engines and constant volume chambers. Budde [3] investigated the interaction between injection timing and fuel adhesion, and retarding the post fuel injection increased the fuel adhesion 30%, while splitting post fuel injections decreased this rate to nearly zero at a significant lower injection quantity condition. A more complicated multidimensional modelling of spray impingement was reported by Andreassi and Ubertini [17]. Fuel density, temperature, engine speed, injection pressure, and injection duration were the parameters in these simulations. The results suggest that increases in density, temperature, and engine speed are causes of decreases in penetration distances, spreading angles, and velocities, and increases in injection pressure reduce penetration but widen the spreading and increase penetration velocities. Changes in injection duration had no obvious influence on the spray characteristics.

The behavior of multi-stage injection was investigated experimentally by Arai and Amagai [18]. High speed visualization of spray behavior and correlation analysis of spray density fluctuations were used in that investigation.

According to previous research, the fuel of the post injection is a cause of the engine oil dilution due to the fuel spray penetration to the cylinder wall, however only the fuel film adhesion and the mechanism of the fuel flow down to the cylinder-piston crevice has been investigated. In this paper, the diesel fuel spray behavior and wall impingement of the post fuel injection under different conditions were investigated with a constant volume chamber by optical access. Further, the fuel adhesion on the cylinder wall and the fuel wall-flow to the piston-cylinder crevice in these conditions was quantified using a precision balance, and the oil dilution mechanism and reduction of the fuel adhesion are discussed.

Experimental

Experimental Setup

The experimental setup is shown in Figure 2. It consists of an optical constant volume chamber, the fuel injection system, the optical observation system, and a controller for these systems. The optical constant volume chamber has a volume of 883 cm^3 (diameter 110 mm, depth 80 mm). The internal structure of the constant volume chamber is shown in Figure 3, it has three windows. Two on the sides of the chamber for the high-speed photography of the spray wall impingement, and one is at the bottom of the chamber and is for the LIF

photography of the images of the wall adhesion plate. The chamber is heated by an electric heater and maintained at 100 °C. A stirring fan is installed at the top of the chamber to be able to agitate the pre-charged gases (ethylene, oxygen, and nitrogen). A set of attachments for the fuel adhesion observations, consisting of a wall adhesion plate, crevice box, and cover, are attached to the stage in the chamber, as shown in Figures 4 and 5. The wall adhesion plate, cover, and crevice box respectively simulate the cylinder liner, piston top surface, and the cylinder- piston crevice of a diesel engine. After fuel spray impingement to the wall adhesion plate in the constant volume chamber, the fuel adheres on the wall adhesion plate, and this is equivalent to the fuel adhesion on the cylinder liner of the diesel engine. In the same manner, the fuels on the cover and crevice box respectively represent the fuel on the piston top surface and the fuel entering the cylinder-piston crevice of the diesel engine. The crevice clearance can be adjusted by sliding the cover. In an actual engine, the relative locations of piston and injector change with the post injection timing, and the relative location of crevice box and cover attachment in the chamber is also changed for the different injection timings.

The pressure in the chamber is measured by a pressure transducer equipped on the inside wall of the chamber, and the temperature at the diesel fuel injection is calculated from the pressure and in-cylinder gas compositions of CO_2, H_2O and N_2 gases produced by the ethylene combustion.

The fuel injection system is powered by an oil pump and a hydraulic amplifier. A Denso G3P injector (piezo injector, f=0.090 mm x 9 holes with a spray angle of 155°) is used in the experiments. The nozzle holes were fluid polished. To observe a single fuel plume, an injector cap is attached at the injector tip by using a microscope, as shown in Figure 6. With this cap, only one nozzle hole (designated nozzle hole) is open to the constant volume chamber, enabling single spray injections. To avoid interference of the other fuel sprays, the injector cap is filled with an absorbent to absorb the fuels from the 8 nozzle holes not open to injecting fuel during the experiments. The space volume where the injected fuel stays inside the injector cap is almost 0.5 cm^3.

Calibration of Fuel Injection Quantity

The fuel injection quantity is precisely measured and strictly controlled in all of the following experiments. For the single injection quantity measurement, the experiments used 500 fuel injections into a closed can at intervals of 100ms, each injection is clearly separate and is

not affecting or affected by other fuel injections, and the average fuel quantity per injection is measured with a precision balance; and the injections take place as suggested in Figure 7. Then, the fuel was also injected from a nozzle hole with injector cap (designated nozzle hole) into a small closed can for 20 times and the fuel injection quantity per one injection was measured by precision balance. The error between the fuel injection quantities of the designated nozzle hole and one ninth of total fuel injection was less than 0.5%.

From now on, the fuel injection quantity from the designated nozzle hole is calculated with one ninth of the mass delivered of the unmasked injector. The measurement is conducted with high precision, and the electric pulse signal durations given to the EDU for 0.6, 1.1, and 1.7 mg were decided.

The fuel quantity of the multi-stage injection is measured in a similar manner to that of the single fuel injection quantity measurements, and the fuel quantity calibration of the multi-stage injection is conducted with a 1.5 ms injection interval condition, as shown in Figure 8.

Optical Observations of Spray Penetration, Impingement, and the Fuel Wall-flow Phenomenon by the Shadowgraph and Mie Scattering Methods

The optical arrangements for the shadowgraph and Mie scattering observations is shown in Figure 9. For the shadowgraph, a 800W Xenon arc is used as light source, and a 6W (max output 8W) YAG laser with a beam of continuous output at wave length 532nm is used as the light source for the Mie scattering observations. A high-speed video camera (NAC image technology GX-8) is used in the experiments with a frame speed of 40,000 fps and 240x240 pixels per image.

Measurements of the Fuel Film Adhesion Area and Thickness on the Wall Adhesion Plate by Laser Induced Florescence Method (LIF)

According to laser induced fluorescence theory, the intensity of the fluorescence induced by a laser depends on the density of the fluorescence agent at the area and the laser light intensity. When the concentration of fluorescence in the oil or fuel and the input laser light intensity are constant, the observed fluorescent light intensity can be determined by the oil and fuel film thickness (Equation 1), and the calibration curve of the fluorescence intensity of the fuel film thickness at room temperature is shown in Figure 10.

$$I = I_0 K(\lambda) F(T, \lambda) Ch \quad (1)$$

I: Observed fluorescence light intensity;

I_0: Input laser light intensity;

K(λ): Function for the laser wavelength;

F(T, λ): Function of the temperature of the fluorescence agent;

C: Density of the fluorescence agent in the fuel;

h: Thickness of the fuel film.

However, the fuel film temperature changes during combustion, fuel injection, and cooling processes, and the influence of *F(T, λ)* in Equation 1 cannot be ignored and must be identified. In the tests, the binarized LIF image is used to obtain the fuel adhesion area on the wall adhesion plate; the mean thickness *h* is obtained from the adhesion area measured by LIF and the mass of the adhering fuel measured by a precision balance as in Equation 2.

$$h = \frac{m}{\rho S} \quad (2)$$

m: Mass of fuel adhesion on the wall adhesion plate

ρ: Density of fuel

S: Fuel adhesion area

The arrangements for the LIF measurements are shown in Figure 11. Laser light is set to a specified angle to the LIF window of the constant volume combustion chamber, while the LIF camera is on the line extending from the point of adhesion on the plate to the LIF window. A dichroic mirror is placed between the LIF camera and the window to reflect and separate the laser light and the fluorescence light of the fluorescence agent rhodamine-B. The laser is the same laser as that used in the Mie scattering observations and at a 3W output. The LIF camera (PCO.edge, sCMOS) records 2560x2160 pixel images at 100 fps.

Fuel

The fuel used in the following tests is the #2 Japanese diesel fuel classified by JIS K2204 specifications which is commercially available. The properties of the fuel are shown in Table 1.

Precision Balance

To measure the weights of wall adhesion plate, cover, and crevice box before and after fuel injection, the precision balance (METTLER TOLEDO MX5) is used. The maximum weighting

capacity is 5000 mg, and its resolution is 1.0 μg (0.001mg). The wall adhesion plate, cover, and crevice box are designed to be less than 3500 mg respectively. The measurement is conducted under the constant temperature and stable condition.

Test Methods and Conditions

To create similar pressure and temperature conditions as those of an actual engine in the constant volume chamber, nitrogen, ethylene, and oxygen gases were introduced into the constant volume chamber and agitated by the stirring fan. When the gas is sufficiently mixed, it is ignited by a spark plug and eventually cooled due to the heat loss through the chamber wall and the glass window. The pressure is monitored by a pressure sensor and the temperature inside the chamber is calculated by the gas state equation. By adjusting the initial pressure and the proportion of nitrogen, ambient temperature and pressure similar to those of the engine can be achieved during the cooling process, as shown in Figure 12. Post fuel is injected when the pressure reaches a target pressure. During this cooling and post fuel injection process, the chamber wall and the stage inside the chamber are maintained at 100°C. The mixture of ethylene and oxygen is maintained at an ideal equivalent ratio (λ=1.0), and combustion does not occur when the diesel fuel is injected. After the fuel spray impingement on the wall adhesion plate is achieved, the cooling system is triggered to cool the stage and the exhaust system operated to prevent adhesion of water vapor on the wall adhesion plate, crevice box, and cover. Then the attachment of the wall adhesion plate, crevice box, and cover are removed from the stage, and disassembled into three pieces, and the mass increase of each part is measured by a precise balance.

Test 1: Effects of the Lubricant Oil Film Adhering on the Cylinder Wall on the Post Fuel Impingement and Adhesion

In an engine, a thin film of lubricant oil is formed on cylinder wall. To investigate the effects of the oil film on the fuel spray impingement and adhesion, post fuel injection to the wall adhesion plate with a lubricant oil film (wet) was performed; and also as a control test, post fuel injection on a dry wall adhesion plate. In the wet test, the lubricant oil film was created by applying the lubricant oil film with an airbrush and masking sheet as shown in Figure 13. The masking sheet has a 30 mm diameter opening and covers the wall adhesion plate (Diameter 50mm). For the lubricant oil application, the airbrush was kept at the same position about 100mm above the masking sheet. Due to the high viscosity of the lubricant oil, 10% of

solvent was mixed into this oil. Further, 0.1% rhodamine-B, a fluorescence agent was mixed into the oil to observe the condition of the lubricant oil film by LIF. After the lubricant oil mixture with solvent and rhodamine-B was applied to the plate, it was placed in a thermostat oven at 60°C for 5 minutes to evaporate the solvent and a thin lubricant oil film is formed on the surface of the wall adhesion plate. The mass increase of the plate after the lubricant oil film application was measured by the precision balance, and the film thickness was calculated from the mass increase, the applied area, and the oil density ($\rho \approx 8.5*10^3$ kg/m^3). It was confirmed that the thickness of the oil film using this method is reproducible and stable with an average 1.02 μm thickness (0.61 mg), as shown in Figure 14. For the observations, the camera is set at 2 fps and the exposure time of 10 ms. Post fuel injections in Test 1 were conducted at the pressure and temperature conditions of 30 °CA ATDC, 60 °CA ATDC, and 90 °CA ATDC of the diesel engine operation at 2000 rpm engine speed. These crank angle conditions are the post fuel injection timings commonly used in diesel engines. The temperature, pressure, and density at these crank angles, and the fuel injection quantities are listed in Table 2.

Test 2: Observation of Spray Penetration, Wall Impingement Behavior, and the Optical Analysis of the Fuel Adhesion Area and Mean Thickness Measurements at the Different Post Fuel Injection Timings

The observations of spray impingement behaviors on the wall were conducted by both of the shadow-graph and Mie scattering methods described above in the optical assessments. For the observation of spray wall impingement, the JIS#2 diesel fuel listed in Table 1 was used. The optical measurements of the fuel adhesion area were conducted by the LIF method. The fuel used for the LIF analyses is the JIS#2 fuel mixed with 0.05% rhodamine-B and 5% ethanol mass proportions. The post injection conditions, pressure, temperature, and density of 30, 60, and 90 °CA ATDC, and with injection quantities of 0.6, 1.1, and1.7 mg/hole are the parameter variables of this test, as shown in Table 3. As the intensity of LIF image is a temperature dependence, the LIF images were only used to measure the fuel adhesion area on the wall adhesion plate. The mean fuel thickness on the wall adhesion plate is obtained from the adhesion area measured by LIF and the mass of the adhering fuel measured by a precision balance as in Equation 2.

Test 3: Quantification of the Fuel Adhering to the Wall and the Fuel Flowing Down (Wall-flow) to the Piston-cylinder Crevice at Different Post Fuel Injection Timings

The test detailed in this section was conducted 10 times and the quantities were averaged to establish the fuel adhering on the cylinder wall. The fuel wall-flow entering into the piston-cylinder crevice was investigated at different post injection timings. The test conditions of Test 3 are the same as in Test 2, and as shown in Table 3. The fuel adhering on the wall and the wall-flow to the piston-cylinder crevice were captured by the fuel adhesion attachment described in the experimental setup section, the wall adhesion plate, the crevice box, and the cover, as shown in Figures 4 and 5. The piston-cylinder crevice clearance is set to 0.4 mm, as measured in a real diesel engine with consideration of the thermal expansion of the piston. After the post fuel injection and exhausting the chamber, the fuel adhesion attachment is removed from the stage of the chamber. To avoid the influence of room temperature variations and human operation during the measurements, all mass measurements were conducted after the fuel adhesion attachment was cooled to the same temperature and all human operation steps were restricted by a time limitation to maintain the exposure time to the room ambient temperature to be the same in all the tests.

Test 4: Effects of Crevice Width between Piston and Cylinder on the Fuel Wall-flow Entrainment Quantity at the Crevice

In Tests 2 and 3, the fuel flow down to the piston-cylinder crevice was observed and quantified. The test discussed next was conducted to investigate the effect of the width of the crevice between piston and cylinder on the wall flow fuel quantities entering into the crevice. The test conditions are shown in Table 4. The injection quantity, pressure, temperature, and density were maintained at 1.1 mg/hole, 0.4 MPa, 590 K, and 2.4 kg/m^3 (60 °CA ATDC condition) respectively, and the width of the crevice was changed from 0.05 to 0.6 mm. The method of this test is the same as in Tests 2 and 3. The optical observations were made using the shadow-graph and Mie scattering methods and the fuel adhered on the adhesion attachment was measured using the precision balance.

Test 5: Effects of Boost Pressure and Engine Load on the Fuel Wall Adhesion Quantity

In actual engine operation, the in-cylinder density changes when the engine is boosted by a supercharger or a turbocharger, and the in-cylinder temperature changes as the engine load increases. The effects of boost pressure and engine load on fuel adhesion on the cylinder

wall were investigated with the constant volume chamber. In Table 5, the boost pressure test, the variable parameter is the density (and pressure), and the in-cylinder temperature was maintained at 500 K. Here 1.1 mg/hole of post fuel was injected and the mass of the wall adhesion plate was determined. In Table 6, the engine load test, the variable parameter is the in-cylinder temperature (and pressure), and the density was maintained at 1.4 kg/m^3. The 1.1 mg/hole of post fuel was injected and the weight of the wall adhesion plate was determined. In both tests, the spray penetration and structure were observed by shadowgraph and Mie scattering methods.

Test 6: The Spray Impingement Behavior and Fuel Adhesion on the Cylinder Wall with Multiple Post Fuel Injections

To minimize the oil dilution, the effects of multiple post fuel injections on the fuel adhesion was investigated. The test temperature and pressure conditions were the same as at the 60 °CA ATDC condition. Different from actual engine operation, there is no piston motion in the chamber, so the pressure drop is significantly slower than the in-cylinder pressure of an engine.

The injection strategy is detailed in Figure 15 and Table 7. The injection quantity is maintained at 0.98 mg, and 0.49 mg/hole or 0.33 mg/hole was injected for each of the two- and three-stage injections. The injection interval between each multiple was set at 1.5 ms that is equivalent to 18 °CA at 2000 rpm of engine speed.

Results and Discussion

Test 1: Effects of the Lubricant Oil Film on the Cylinder Wall on the Post Fuel Impingement and Adhesion

This test detailed above was conducted 10 times and averaged, with the fuel adhesion quantity measured by the precision balance. The results of fuel adhering on the wall with a 1μm lubricant oil film is shown in Figure 16, and plotted with the test results of fuel adhesion on the dry wall. The results show that less fuel spray is measured on the wall with the lubricant oil film than on the dry wall, and the effects of the oil film increase with increasing delay in the post fuel injection timing.

Figure 16 also shows LIF images of the lubricant oil film layer after the fuel impingement. With the 30 °CA ATDC case, the oil film surface after the fuel injection is flat, and liquid fuel did not reach the surface of the oil layer. At 60 °CA ATDC, there is a small crater at the center

of the lubricant oil film after the post fuel spray impingement, and in the 90 °CA ATDC image, this crater is larger than that at 60 °CA ATDC. From the test results of the quantification and the LIF observations in Figure 16, an oil splash was observed at the impact of the post fuel injection and the fuel penetration to the oil film on the wall adhesion plate increased with the delay in the post fuel injection timing. The force of penetration of the fuel spray impinging on the lubricant oil film blows the oil off from the wall, and this is a cause of the decrease in mass at the later ATDC injections, and causes the increases in the mass measurement error of adhering fuel. To avoid the effect of the oil blowing off by the fuel spray, the following tests were conducted with the dry wall condition.

Test 2: The Observations of Spray Penetration, Wall Impingement Behavior and the Optical Analysis of the Fuel Adhesion Area and Mean Thickness Measurements at Different Post Fuel Injection Timings

Images of spray penetration and wall impingement at different timings after the post fuel injection, using the shadow-graph and Mie-scattering methods at 30 °CA ATDC are shown in Figure 17. The fuel is injected to the corner of the cylinder wall (adhesion plate) and the piston top (crevice cover). In the Mie scattering images of 0.6 mg and 1.1 mg fuel injections, the liquid fuel does not reach the surface of the wall adhesion plate, and in the shadow graph images the fuel is vaporized at the spray plume tip and the gas phase fuel hits the wall adhesion plate. With the increase in fuel injection quantity up to 1.7 mg, the liquid fuel of the spray plume tip slightly hits on the wall adhesion plate in the Mie scattering images.

The optical observation images of the post fuel injection behavior at 60 and 90 °CA ATDCs are shown in Figures 18 and 19. Compared with the images at 30 °CA ATDC in Figure 17, the post fuel injections at these timings clearly show liquid fuel spray wall impingement and fuel spreading on the cylinder wall with the stronger penetration, this is caused by the in-cylinder pressure and temperature being lower at the later post fuel injection timing. The penetration of liquid and gas phases of 1.1 mg of post fuel injection is shown in Figure 20. At the 30 °CA ATDC condition, the in-cylinder pressure and temperature are the highest of the three, and the liquid fuel does not reach the wall adhesion plate. The fuel vaporizes and only gaseous fuel reaches the wall adhesion plate. As the post fuel injection timing is delayed from 30 to 90 °CA ATDC, the fuel penetration reaches further and both liquid and gas phases of the fuel simultaneously impinge on the wall adhesion plate.

The results of the optical analysis of the fuel adhesion area by the LIF method and the mean

thickness of the adhering fuel are shown in Figure 21. The black and white photos show the LIF images of 0.6 mg/hole (left) and 1.7 mg/hole (right) fuel injections. At 30 °CA ATDC, the area with adhesion is large despite the weak spray penetration, however, the mean thickness of the fuel film is very thin, less than 1μm. The test results suggest that vaporized fuel has condensed on the surface of the wall adhesion plate and that a thin fuel film adhered widely on the wall adhesion plate. At 60 °CA ATDC, the fuel adhering area is the smallest of the three investigated, however the mean thickness of the fuel film is the thicker of these. With the higher injection quantity, the area of fuel adhesion and the film thickness increases. At 90 °CA ATDC, a thick and wide fuel film is adhering on the wall adhesion plate, due to the large amount of fuel spray impingement. As the fuel injection quantity increases, the fuel film thickness increases greatly while the adhering area remains very similar.

In both the fuel injections at the 60 and 90 °CA ATDC conditions, the wall-flow, which is a high speed liquid phase flow towards the cover and crevice box, is observed, and further details will be discussed with Test 3 below.

Test 3: Quantification of Fuel Adhering to the Wall and Fuel Flowing down (Wall-flow) to the Piston-cylinder Crevice at Different Post Fuel Injection Timings

The results of the quantification of fuel adhesion quantities to the different parts of the fuel adhesion attachment are shown in Figure 22 and the fuel adhesion percentage versus the injection quantity is shown in Figure 23. In both bar graphs, the fuel adhering to the wall adhesion plate (red), cover (orange), and crevice box (blue) show the ratio of the fuel adhering to the cylinder wall, the fuel adhering to the piston surface, and the fuel which entered the piston-cylinder crevice respectively, as explained in Figures 4 and 5. As shown in Figure 5, the post fuel at 30 °CA ATDC is injected directly into the cylinder-piston crevice, however most of this post fuel vaporizes before the impingement and only a little of the mass takes part in the wall-flow in Figure 22. At the 60 and 90 °CA ATDC conditions, liquid phase wall-flow on the piston and crevice can be observed in the video images of Figures 18 and 19, however the test results in Figure 22 show that this wall-flow vaporizes before it reaches to the piston top and crevice. As a result, the total wall-flow mass on the piston and in the crevice (orange and blue) are small and similar in all test conditions. These results clearly show that the fuel adhering to the wall (red in Figure 22) is the main cause of the oil dilution. In Figure 23, the adhesion percentage increases as the post fuel injection timing becomes later, however, at the same injection timing, the fuel adhesion percentage decreases with

increases in the fuel injection quantity. This may be interpreted to show that there is a saturation limit for fuel that adheres to the wall. During the injection, the fuel first adheres on the surface of the wall adhesion plate, however the following fuel impinges the fuel on the wall adhesion plate and the adhered fuel is splashed. The balance of fuel adhesion and splash may decide the saturation limit for fuel that adheres to the wall.

Test 4: Effects of Crevice Width between Piston and Cylinder on the Fuel Wall-flow Entrainment in the Crevice

The effects of crevice width on wall-flow mass percentages are detailed in Figure 24. The experiments in all conditions here are also repeated 10 times and the results show averages with error bars indicating the maximum and minimum values in 10 times experiments. The fuel injection quantity is 1.1 mg/hole, and the tests were conducted at the 60 °CA ATDC condition (0.4 MPa, 590 K, and 2.4 kg/m^3).

The quantity of fuel entering the piston-cylinder crevice was less than 5% of the total injected quantity in all cases. This result suggests that the quantity of fuel entering the crevice does not simply increase with the width of the crevice. When the width is smaller than 0.20 mm, the quantity of fuel entering the crevice increased as the crevice width decreased, however, with crevice width larger than 0.20 mm the quantity of fuel entering the crevice increased. From the observation of the spray behavior in Test 2, the fuel layer of the wall-flow has a thickness of 1.5 mm and it was considered that the fuel quantity increased as the width of the crevice increases, however the reason for the increasing volume of fuel entering the crevice when the width decreased to 0.05mm cannot be explained from the observed images. Speculatively, one reason for this phenomenon could be that there is a capillarity effect when the width of the crevice is smaller than a specific value between 0.20mm and 0.05mm.

Test 5: Effects of the Boost Pressure and Engine Load on the Fuel Wall Adhesion Quantity

The effect of the boost pressure by supercharging on post fuel adhesion was investigated and will be detailed here. The variable parameter here is the in-cylinder density (boost pressure) and the in-cylinder temperature was maintained at 500 K, with 1.1 mg of post fuel injected. Figure 25 shows shadow graph images of the test results. The spray cone angle becomes wider and the penetration of fuel spray becomes shorter with increases in the boost pressure (density). The experiments in all conditions are repeated 10 times and Figure 26

shows the average quantity adhering to the wall adhesion plate measured by the precision balance. Each error bar indicates the maximum and minimum values in 10 times experiments. The adhering fuel quantity decreases with the increase in in-cylinder pressure and this suggests that boosting the pressure is effective in lowering post fuel adhesion on the cylinder wall.

The effects of the engine load on the post fuel adhesion were also investigated. The variable parameter here is the in-cylinder temperature, varied from 500 to 800 K, and the in-cylinder density was maintained at 1.4 kg/m^3, here 1.1 mg of post fuel was injected and the images of the spray are shown in Figure 27. In all cases, the liquid fuel impinges on the wall adhesion plate, but with increases in the in-cylinder temperature the spray cone angle becomes narrower, and there is less liquid fuel spreading. The experiments in all conditions are repeated 10 times and the average quantities of fuel adhering to the wall are plotted in Figure 28. Each error bar indicates the maximum and minimum values in 10 times experiments. The fuel quantity adhering to the wall decreases when the ambient temperature increases. This result suggests that post injection at medium engine loads reduces the post fuel adhesion quantity on the cylinder wall and the engine oil dilution rate.

Test 6: Spray Impingement Behavior and Fuel Adhesion on the Cylinder Wall with Multiple Post Fuel Injections

Here the injected fuel quantity is maintained at 0.98 mg, and 0.49 mg or 0.33 mg of fuel is injected in each of the injections of the two- and three-stage injections. The interval between multiple injections was set at 1.5 ms. The experiments in all conditions are repeated 10 times. The plots in Figure 29 show the total fuel adhesion percentage in the multi-stage injections and each error bar indicates the maximum and minimum values in 10 times experiments. The total fuel adhesion percentage decreased with the increase in the number of injections. Figure 30 shows images of a single injection spray, the second spray of the two-stage injection, and the third spray of three-stage injection 0.5 ms after the start of injection (SOI). For the single injection, 0.98 mg of fuel is injected and there is much impingement on the cylinder wall, however for the two- and three-stage injections, the fuel quantity per injection is half (0.49 mg) and one-third (0.33 mg) of the single injection, and the fuel is vaporized before impingement because the heat capacity in each fuel injection becomes smaller with increase in the number of fuel injections. This is a reason why the fuel adhesion percentage of the multi-stage injection becomes smaller with increases in the number of fuel injections

in Figure 29.

Figure 31 shows Mie scattering and shadow graph images of the three-stage injection with the 1.5 ms intervals between the injections. The figure suggests that the fuel penetrates further with the increase in injection number. Figure 32 shows the residual spray flow speeds of first and second fuel injections just before the second and third fuels are injected. The residual spray flow speed is measured at 9 positions along the spray. The first fuel spray vaporizes before the spray hits the cylinder wall and the inertia motion of vapor flow to the wall remains in the spray pass. The average speed of the residual motion in the nine positions of the first injection at the start of second injection was 4.73 m/s, and that of second injection at the start of third injection was 5.62 m/s. When the second and third fuel injections take place, the vapor flow motion of the previous injection furthers the spray flow of the following fuel injection by a slipstream effect, and this is why the fuel penetration increases with the increase in the number of injections in Figure 31. The effects on fuel impingement by the temperature drop in the in-cylinder volume that the spray passes due to fuel vaporization were investigated by CFD simulations, however the results show that the temperature recovers before the second and third fuel injections, because of the large heat capacity of the environment in the cylinder.

These results suggest that the multiple fuel injection is effective to reduce of fuel adhesion on the cylinder wall, however the length of the fuel penetration increases with the increase in the number of the injections because of the presence of previous spray motion (turbulence).

Conclusions

In this research, the spray wall impingement of post fuel injections is observed by optical methods, and the fuel adhesion to the cylinder wall and the fuel flow entering the piston-cylinder crevice caused by post fuel injection is investigated. The conclusions of Tests 1 to 6 conducted in a constant volume chamber may be summarized as follows:

1. In the early post fuel injection at 30 °CA ATDC, the fuel spray evaporates and almost only gas phase impinges on the wall with a large spray cone angle and weak penetration. The fuel adhering on the wall is mainly condensed gas fuel and this is cause of the large area of adhesion with a thin fuel film. The fuel flow entering the piston cylinder crevice is also in the gas phase and condenses in the crevice.
2. As the injection timing becomes later, the liquid phase proportion in the fuel spray increases resulting in further penetration because of the lower temperature and pressure

in the cylinder. The effect of the liquid fuel impinging on the wall increases and results in a thicker fuel film across a larger area. Liquid fuel diffusion near the wall was confirmed, and a part of this enters the piston cylinder crevice.

3. At all injection quantity conditions, fuel wall adhesion increases as the injection timing becomes later. At the same injection timing, fuel adhesion to the wall increases as injection quantity increases while the fuel adhesion percentage at the wall decreases. At all conditions, it was confirmed that there is wall flow of fuel entering the crevice, however fuel adhering to the wall is the main cause of the lubricant oil dilution.
4. The amount of fuel entering the piston-cylinder crevice changes with the width of the crevice. The quantity of fuel entering the crevice increases when the crevice is either very wide or very narrow. From the test results obtained in this, there is an optimal width of the piston-cylinder crevice which suppresses the wall flow of fuel entering the crevice to a minimum quantity.
5. The mass of fuel adhering to the wall caused by the post fuel injection decreases when the in-cylinder density or the temperature increase. This suggests that post injection at high boost pressures and higher engine loads slows the oil dilution rate.
6. Multiple fuel injections is effective to reduce fuel adhesion on the cylinder wall, however the distance of the fuel penetration becomes longer with increases in the number of injections, because of the turbulence from previous sprays.

Acknowledgements

This research is one of the projects promoted by the Research association of Automotive Internal Combustion Engine (AICE) and financially supported by the Japan Ministry of Economy, Trade and Industry, and the auto industry.

References

1. Bouchez, M., and Dementhon, J., "Strategies for the Control of Particulate Trap Regeneration", SAE Technical Paper, 2000-01-0472, 2000
2. Yamamoto, K., Takada, K., Kusaka, J., Kanno, Y., and Nagata, M., "Influence of Diesel Post Injection Timing on HC Emissions and Catalytic Oxidation Performance", SAE Technical Paper, 2006-01-3442, 2006

3. Budde, M., Ehrly, M., Jakob, M., Wittler, M., and Pischinger, S., "Simulation and Optical Analysis of Oil Dilution in Diesel Regeneration Operation", SAE Technical Paper, 2011-01-1844, 2005
4. Deconninck, B., Delvigne, T., Courtois, O., Dequenne, B. et al.", A New Methodology for On Line Oil Dilution Measurement," SAE Technical Paper, 2005-01-2170, 2005
5. Oinuma, R., Takuma, S., Koyano, T., and Takiguchi, M., "Effects of Post Injection on Piston Lubrication in a Common Rail Small Bore Diesel Engine", SAE Technical Paper 2005-01-2166, 2005
6. Wattrus, M., "Fuel Property Effects on Oil Dilution in Diesel Engines", SAE International Journal of Fuels and Lubricants V122-4. 2013-01-2680, 2013
7. Parks, J., Partridge, B., and Whitacre, S., "Rapid in Situ Measurement of Fuel Dilution of Oil in a Diesel Engine using Laser-Induced Fluorescence Spectroscopy", SAE Technical Paper 2007-01-4108, 2007
8. Katsura, N., Saito, M., and Senda, J., “Characteristics of a diesel spray impinging on a flat wall”, International Symposium COMODIA, Vol. 90, pp. 193-198
9. Zhao, L., Torelli, R., Zhu, X., Scarcelli, R. et al., "An Experimental and Numerical Study of Diesel Spray Impingement on a Flat Plate", SAE International Journal of Fuels and Lubricants V126-4, 201701-0854, 2017
10. KO, K., HUH, J., ARAI, M., “Diesel Spray Impingement Behavior and Adhering Fuel on a Recessed Wall. SAE Technical Paper, 2003-01-1834, 2013
11. MURAMATSU, K., et al., “Measurement of Fuel Liquid Film under the Different Injection Pressure”, SAE Technical Paper, 2013-32-9167, 2013
12. YANG, B., GHANDHI, J., “Measurement of Diesel Spray Impingement and Fuel Film Characteristics Using Refractive Index Matching Method”, SAE Technical Paper, 2007-01-0485, 2007
13. Thorsten J., Moller, M., Chaves, H., Obermeier, F., “Fuel Deposition on Wall Impingement of a Spray”, SAE Technical Paper, 961207, 1996
14. Ebara, T., Amagai, K., and Arai, M., “Movement and Structure of Diesel Spray Impinging on an Inclined Wall”, SAE Technical Paper, 970046, 1997
15. Amagai, K., Maruyama, Y., Saito, M., and Arai, M., “Spray-to-Spray Interactions after Wall Impingement”, SAE Technical Paper, 2003-01-1835, 2003
16. Al-Roub, M., Farrell, P., and Senda, J., "Near Wall Interaction in Spray Impingement," SAE Technical Paper 960863, 1996.

17. Andreassi, L., and Ubertini, S., “Multidimensional Modelling of Spray Impingement in Modern Diesel Engines”, SAE Technical Paper, 2005-24-092, 2005
18. Arai, M., and Amagai, K., “Dynamic Behavior of Multi-Stage Injection Diesel Spray”, SAE Technical Paper, 970044, 1997

Table 1. Fuel properties

Fuel	Doesel Fuel (JIS #2)
10% Distillation temp. [°C]	209.5
50% Distillation temp. [°C]	279.0
90% Distillation temp. [°C]	336.5
Density (15°C) [g/cm^3]	0.833
Viscosity (30°C) [mm^2/s]	3.64
Cetane number	52.9

Table 2. The ambient atmospheres in the chamber and injected quantities at the related crank angles in Test 1

Post injection timing [°CA ATDC]	Condition in the chamber at fuel injection			Injection quantity [mg/hole]
	Press. [MPa]	Temp. [K]	Density [kg/m^3]	
30	1.40	810	6.0	1.1
60	0.40	590	2.4	
90	0.19	490	1.4	

Table 3. The ambient atmospheres in the chamber and injected quantities at the related crank angles in Test 2

Post injection timing [°CA ATDC]	Condition in the chamber at fuel injection			Injection quantity [mg/hole]
	Press. [MPa]	Temp. [K]	Density [kg/m^3]	
30	1.40	810	6.0	0.6
60	0.40	590	2.4	1.1
90	0.19	490	1.4	1.7

Table 4. The test conditions of Test 4

Injection timing 60 °CA ATDC			Injection quantity [mg/hole]	Crevice width [mm]
Pressure [MPa]	Temperature [K]	Density [kg/m^3]		
0.40	590	2.40	1.10	0.05
				0.20
				0.40
				0.60

Table 5. The test conditions of ambient density (and pressure effects on fuel wall adhesion in Test 5

Pressure [MPa]	Temperature [K]	Density [kg/m^3]	Injection quantity [mg/hole]
0.19	500	1.4	1.1
0.50		3.6	
0.81		5.8	
1.12		8.0	

Table 6. The test conditions of ambient temperature (and pressure effects on fuel wall adhesion in Test 5

Pressure [MPa]	Temperature [K]	Density [kg/m^3]	Injection quantity [mg/hole]
0.19	500	1.4	1.1
0.24	600		
0.28	700		
0.32	800		

Table 7. The test conditions of multi-stage injection in Test 6

Number of injections [-]	Injection interval [ms]	Injection quantity [mg/hole]	Total injection quantity [mg]	Injection timing [°CA ATDC]
1	-	0.98	0.98	60
2	1.5	0.49		
3		0.33		

60 °CA ATDC condition: 590K, 0.4MPa, 2.5kg/m^3

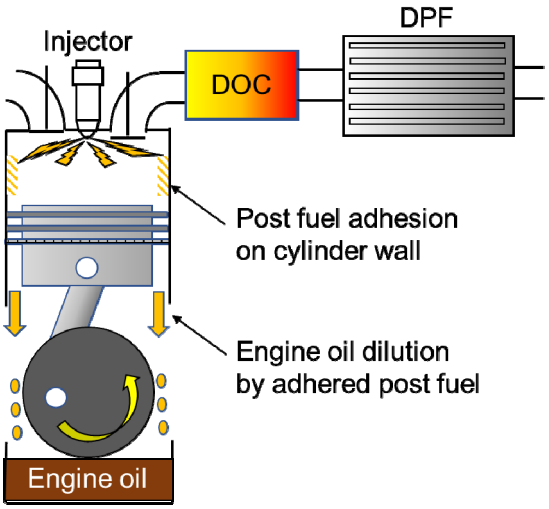

Figure 1. Image of DPF regeneration process

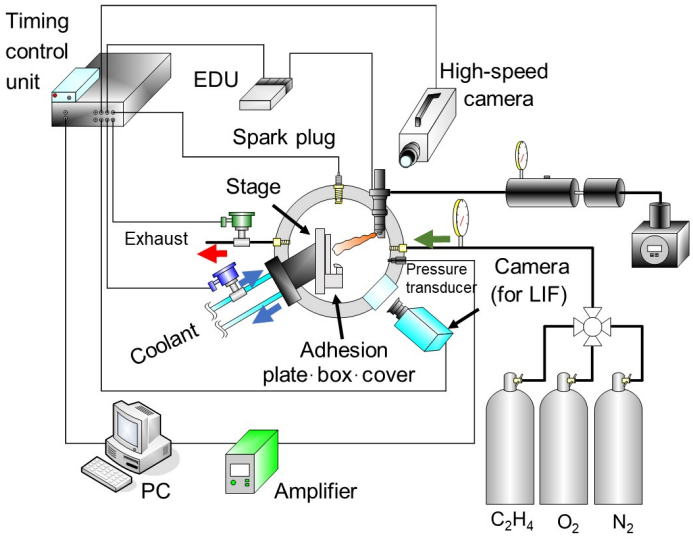

Figure 2. Experimental set-up

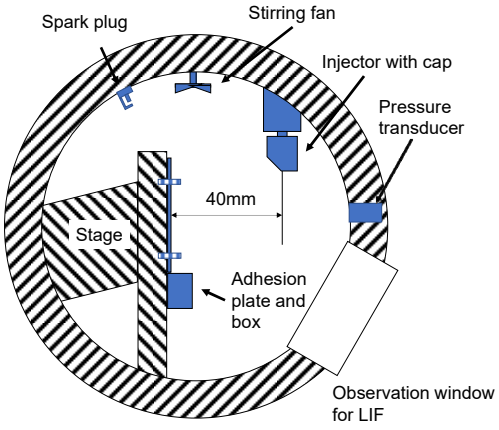

Figure 3. Internal structure of the constant volume chamber

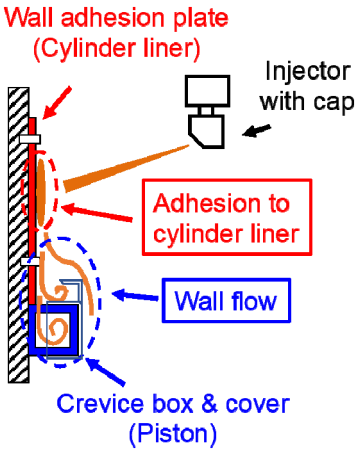

Figure 4. Outline of the fuel adhesion attachment used to measure fuel adhering to the wall and the fuel flow entering the crevice

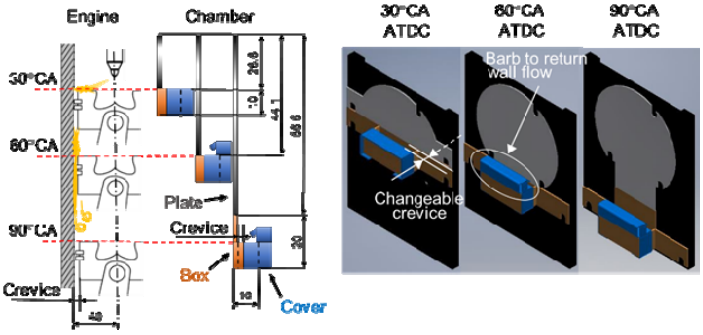

Figure 5. Different fuel adhesion attachments for different crank angles

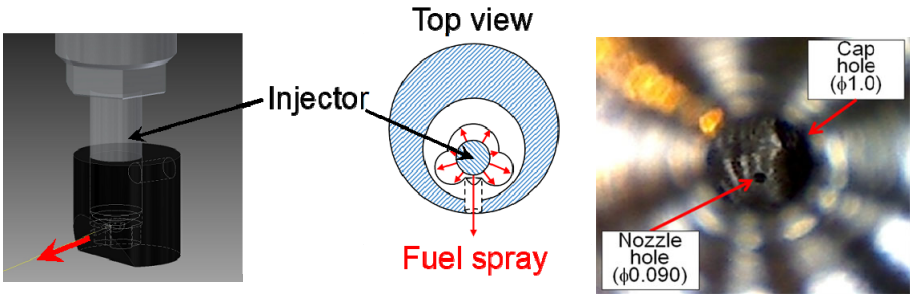

Figure 6. Outline of the injector cap (left and middle) and a microscope image of nozzle hole with injector cap (right)

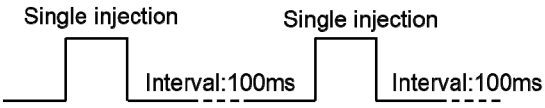

Figure 7. Single injection interval in the injection quantity measurements

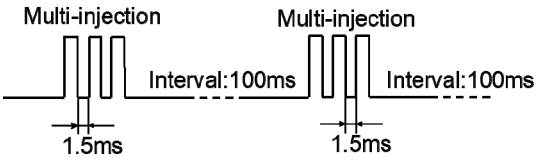

Figure 8. Multi-stage injection in injection quantity measurements

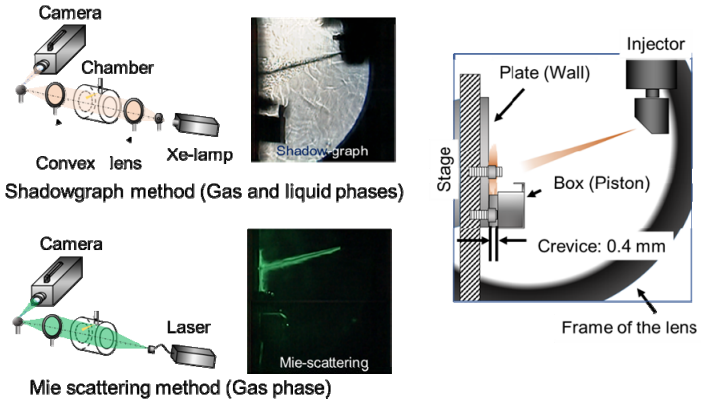

Figure 9. Outline of set-up and images of shadowgraph and Mie scattering observations

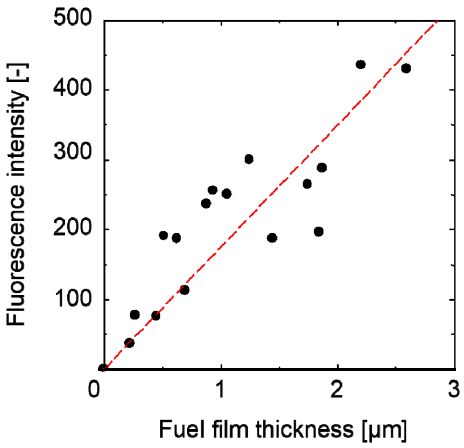

Figure 10. Calibration plot with curve of fluorescence intensity to fuel film thickness at room temperature

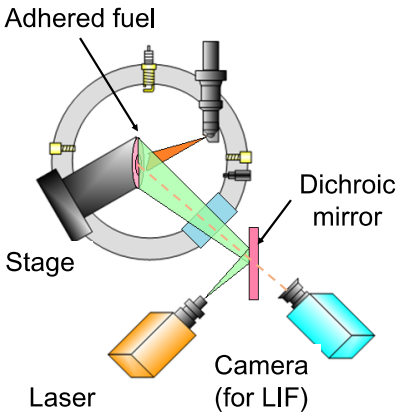

Figure 11. Outline of set-up for the Mie scattering observations

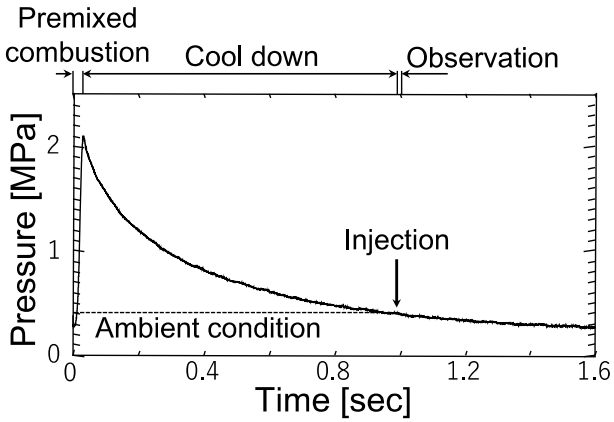

Figure 12. An example of the location of the target ambient atmosphere in the cooling process

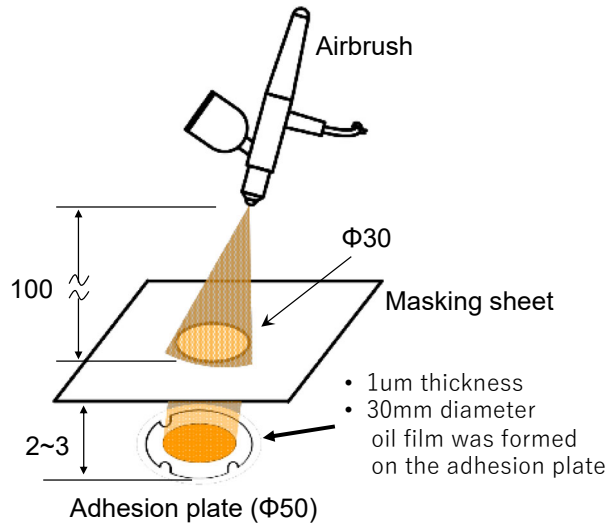

Figure 13. The method of applying lubricant oil film

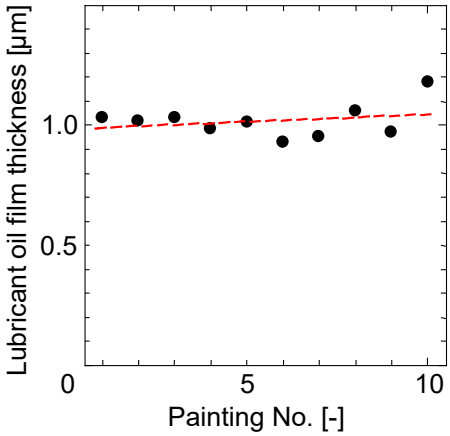

Figure 14. The plot of lubricant oil film thickness

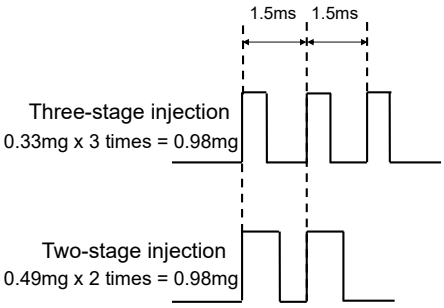

Figure 15. Time interval in multi-stage injections in Test 6

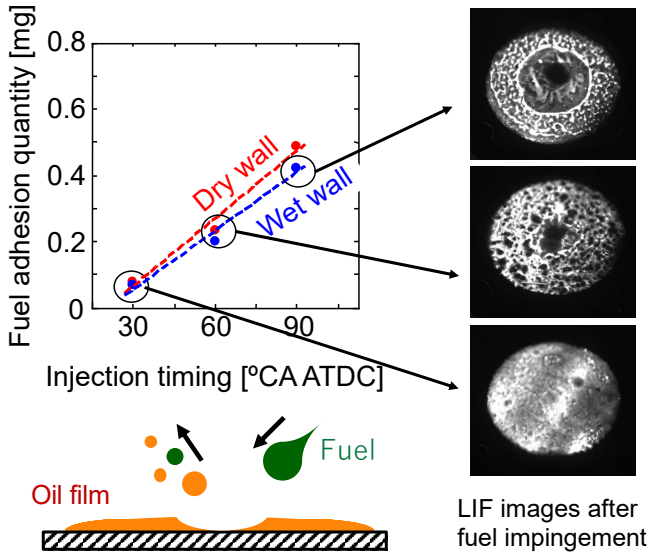

Figure 16. Fuel wall adhesion quantities with and without lubricant oil film (Fuel injection quantity: 1.1mg/hole)

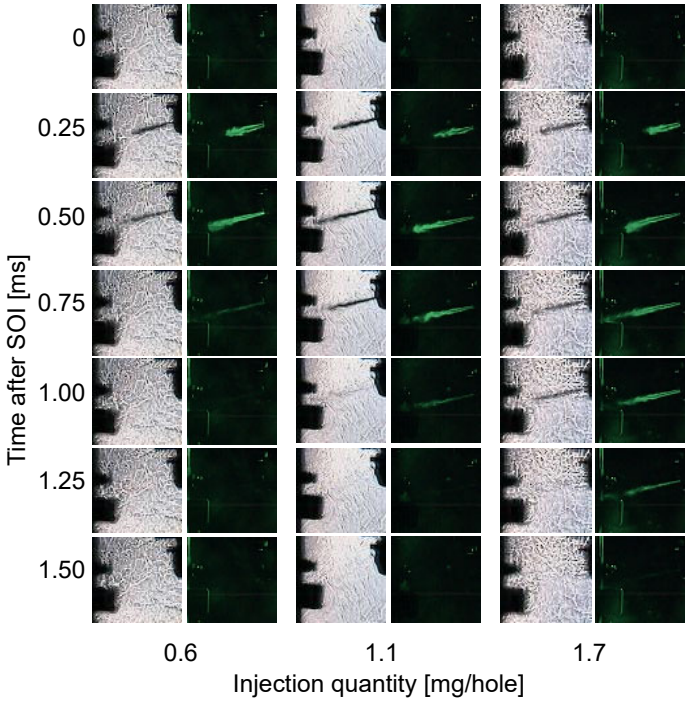

Figure 17. Observation of spray penetration and wall impingement at 30 CA ATDC (left: shadowgraph, right: Mie scattering)

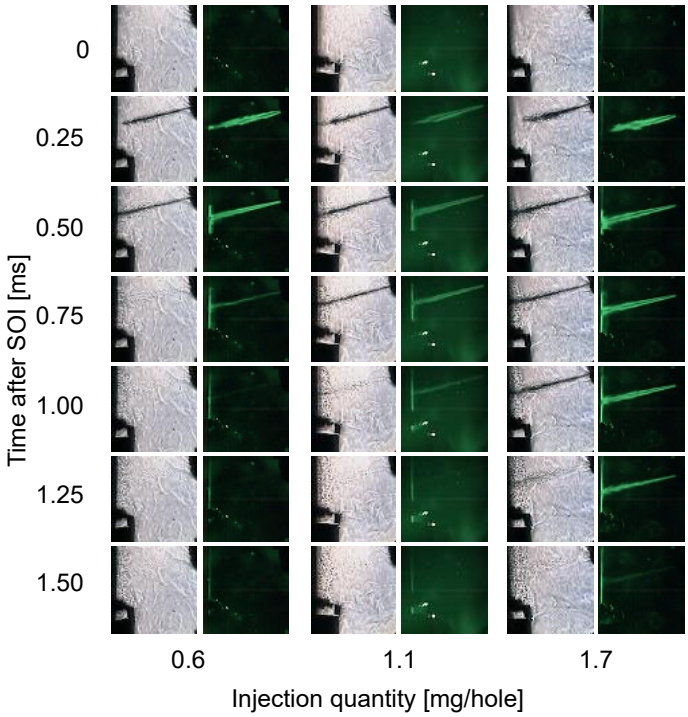

Figure 18. Observation of spray penetration and wall impingement at 60 CA ATDC (left: shadowgraph, right: Mie scattering)

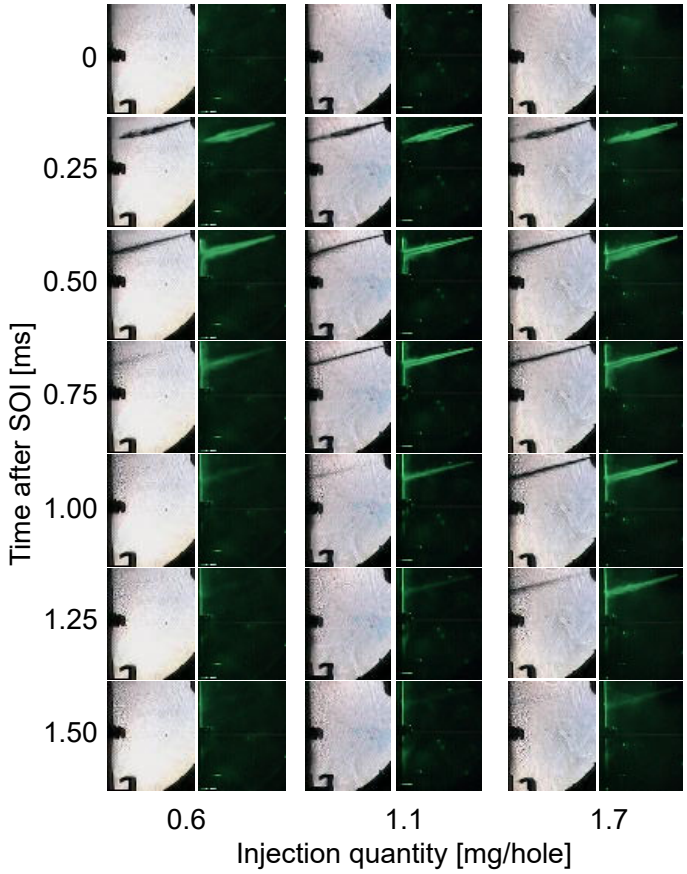

Figure 19. Observation of spray penetration and wall impingement at 90CA ATDC (left: shadowgraph, right: Mie scattering)

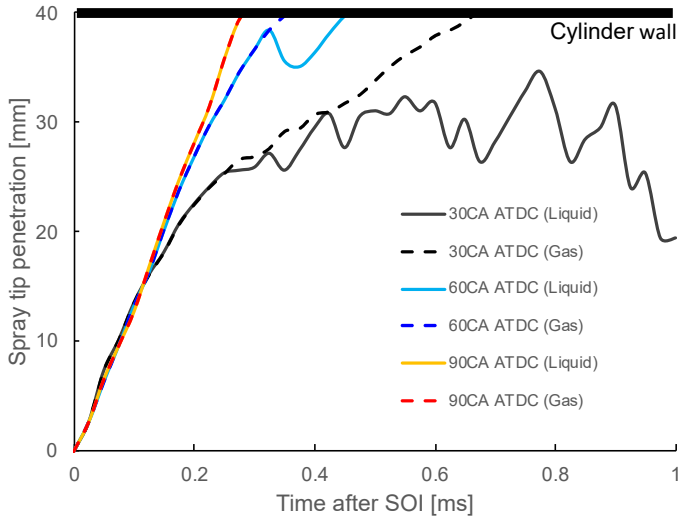

Figure 20. Plots of 1.1 mg fuel spray penetration at 30, 60, and 90CA ATDCs

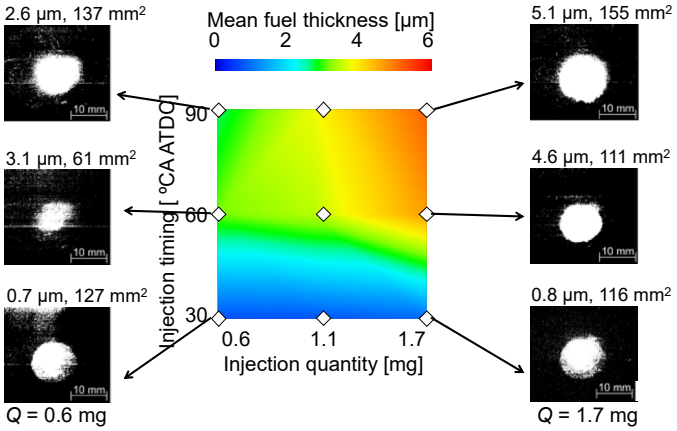

Figure 21. Fuel adhesion area and fuel film mean thickness (Wall adhesion)

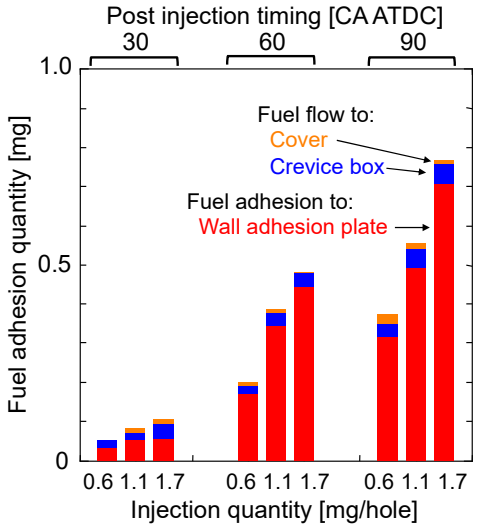

Figure 22. Mass of fuel adhering walls and fuel wall flow entering the crevice

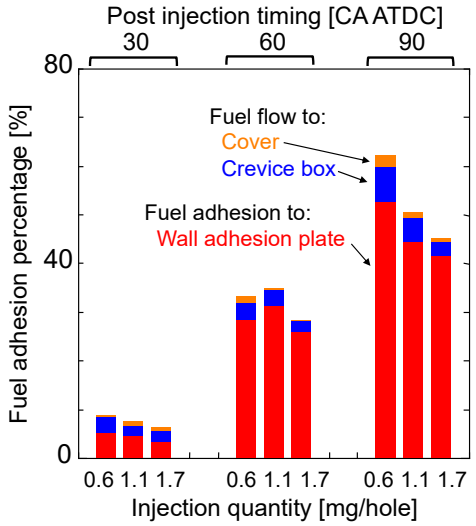

Figure 23. Percentage of fuel adhering walls and fuel wall flow entering the crevice

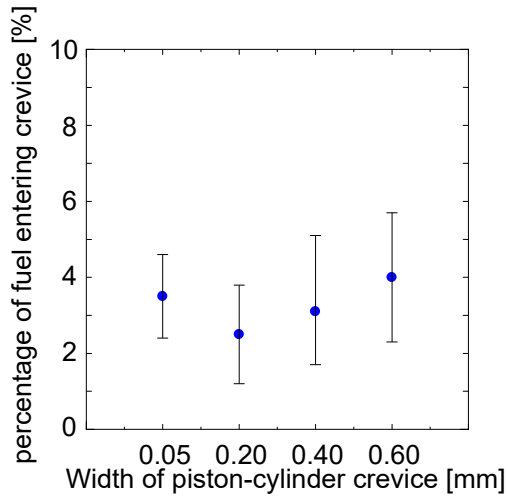

Figure 24. The percentage of fuel entering the piston-cylinder crevice at different crevice widths (injection quantity: 1.1 mg/hole, pressure: 0.4 MPa, temperature: 590 K, density: 2.4 kg/m^3 (60 CA ATDC condition))

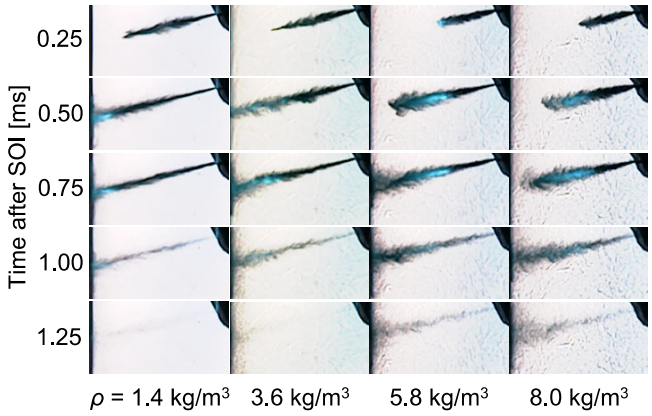

Figure 25. Effect of in-cylinder gas density on fuel spray behavior (test condition as in Table 5)

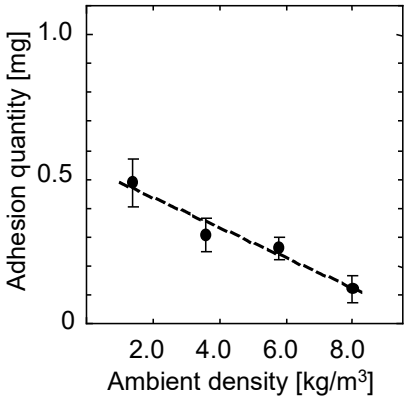

Figure 26. Effect of in-cylinder gas density on fuel wall adhesion (test condition as in Table 5)

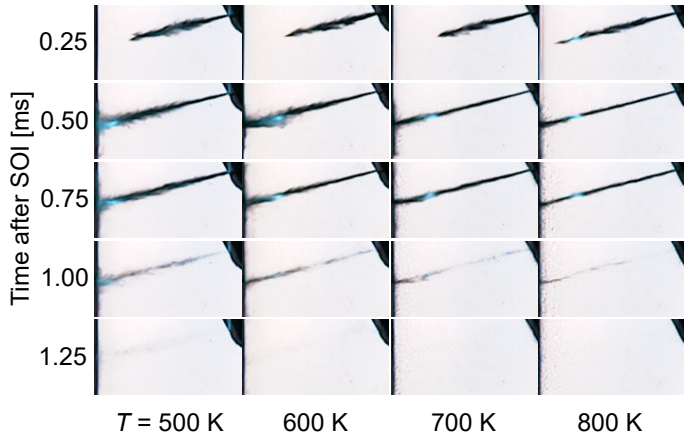

Figure 27. Effect of in-cylinder temperature on fuel spray behavior (test condition is shown in Table 5)

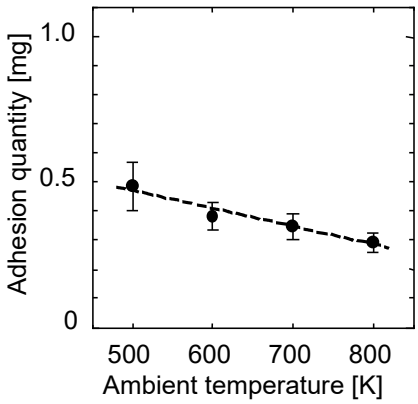

Figure 28. Effect of in-cylinder temperature on fuel wall adhesion

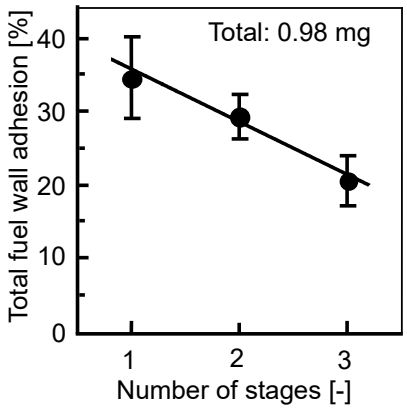

Figure 29. Total fuel wall adhesion percentage in multi stage fuel injection

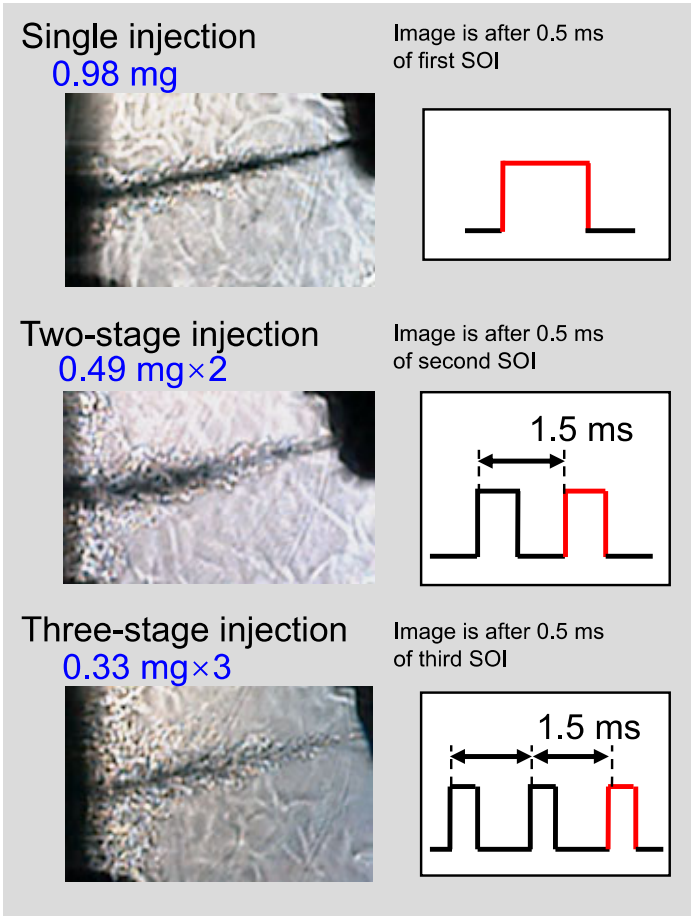

Figure 30. Images of single injection spray, second spray of two-stage injection, and third spray of three-stage injection 0.5ms after the start of injection (SOI)

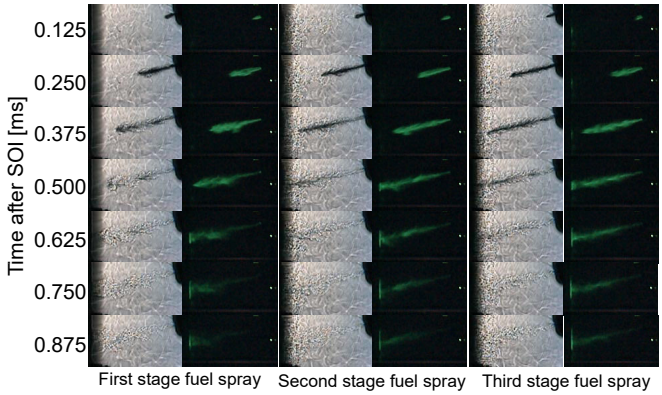

Figure 31. Shadowgraph and Mie scattering images of first, second, and third sprays of three-stage injections

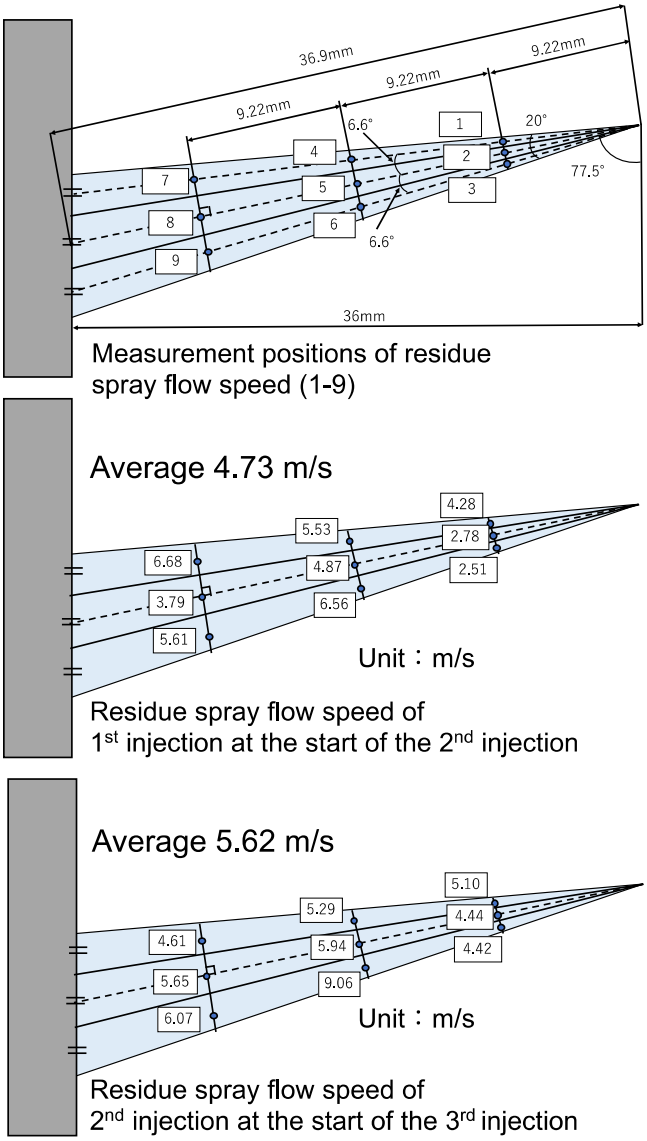

Figure 32. Residue spray flow speed of 1st and 2nd injections at the start of 2nd and 3rd injections